

# Low-Cost, On-Site, Nano-Impact Detection of Silver Nanoparticles via Laser-Ablated Screen-Printed Microelectrodes

Leroy Grob, Lennart J. K. Weiß, Emir Music, Ilja Schwertfeger, George Al Boustani, Julian Feuerbach, Marta Nikić, Lukas Hiendlmeier, Philipp Rinklin, and Bernhard Wolfrum\*

With the ever-growing presence of silver nanoparticles in consumer products, there is a need for cost-effective and on-site monitoring of their influence on our environment. Herein, we report the use of screen-printed and laser-ablated microelectrode arrays (SPMEAs) for the electrochemical detection of 20 nm-sized silver nanoparticles (AgNPs) via collision electrochemistry. The electrodes' morphology is optically analyzed and their electrochemical properties later characterized using cyclic voltammetry and impedance spectroscopy. The SPMEAs are calibrated using a AgNP concentration range of 1 to 100 pM, resulting in a linear dependency of 22 mHz pM<sup>-1</sup> for the impact frequency. Finally, to demonstrate the possibility of future on-site applications, an in-house built portable nanoparticle detection (POND) device is used to measure Faradaic AgNP impacts on a SPMEA, in a solution contaminated with urea.

challenging to know the AgNPs individual fate due to their small size and complex chemical interactions in different environments.<sup>[7]</sup> The increased interest in AgNPs has also in part been due to their size-dependent cytotoxic behavior.<sup>[11,12]</sup> In particular, small AgNPs (i.e. 10 nm) have shown to induce a “Trojan-horse” type mechanism in cells, potentially leading to cellular degradation.<sup>[13–16]</sup> There is therefore a need to monitor the presence of AgNPs in our environment,<sup>[17,18]</sup> and our ecosystems.<sup>[19]</sup>

In order to better understand the impact of AgNPs on the environment, trace analysis of potentially contaminated samples is required. For determining the nanoparti-

## 1. Introduction

Nanoparticles have been increasingly used over the past decades,<sup>[1–4]</sup> without a clear understanding of their impact on the environment.<sup>[5,6]</sup> In particular, there has been a preferential interest in silver nanoparticles (AgNPs) due to their antimicrobial properties.<sup>[7]</sup> For instance, AgNPs have been used in coatings or within fluids on a number of consumer products.<sup>[3,8–10]</sup> However, once these consumer products are in use, it becomes

cles' size, techniques such as electron microscopy (EM), atomic force microscopy, and dynamic light scattering have commonly been used.<sup>[6,7]</sup> In addition to the size of particles, their concentration is also a critical parameter. This is more commonly investigated using element-selective detection techniques such as inductively coupled plasma mass spectroscopy (ICP-MS), ICP-optical emission spectroscopy (ICP-OES), or Raman spectroscopy.<sup>[20,21]</sup> Besides their specific pros and cons, all these techniques lack the possibility of rapid on-site detection. Furthermore, typically they require samples to be transported to centralized lab facilities. This can in turn lead to sample fouling and greatly increase administrative tasks. In order to save time and resources, mobile (pre-)screening techniques would greatly aid in collecting appropriate samples before more in-depth analysis is undertaken. In this regard, electrochemical sensors in combination with a mobile electronic system have shown to be good prescreening platforms for detecting environmental contaminants such as heavy metals.<sup>[22–27]</sup> In fact, the AgNP themselves are known to interfere with their environment and could be the most straightforward sensing target for detecting redox active contaminants.<sup>[28–32]</sup>

To date, there are several methods by which various nanoparticle species can be detected electrochemically.<sup>[33]</sup> In the case of AgNPs, they can be directly detected by using the Faradaic nano-impact approach.<sup>[34–36]</sup> Faradaic nano-impacts involve an electron transfer upon collision of a single nanoparticle at an appropriately biased microelectrode. By applying an oxidation potential, AgNPs can react with halides.<sup>[37]</sup> In turn, an electron

L. Grob, L. J. K. Weiß, E. Music, G. Al Boustani, J. Feuerbach, M. Nikić, L. Hiendlmeier, P. Rinklin, B. Wolfrum  
Neuroelectronics – Munich Institute of Biomedical Engineering  
Department of Electrical Engineering  
TUM School of Computation  
Information and Technology  
Technical University of Munich  
Hans-Piloty-Str. 1, 85748 Garching, Germany  
E-mail: bernhard.wolfrum@tum.de

I. Schwertfeger  
Hoffmann + Krippner GmbH  
Siemensstrasse 1 74722, Buchen, Germany

 The ORCID identification number(s) for the author(s) of this article can be found under <https://doi.org/10.1002/admt.202201880>.

© 2023 The Authors. Advanced Materials Technologies published by Wiley-VCH GmbH. This is an open access article under the terms of the Creative Commons Attribution License, which permits use, distribution and reproduction in any medium, provided the original work is properly cited.

DOI: 10.1002/admt.202201880

transfer occurs and is monitored by an electronic amplifier as a current spike. From the resulting current–time traces, two pieces of information can be gathered: By integrating over the current spike, the charge can be calculated, which in turn relates to the size of the AgNP. In addition, the frequency of current spikes relates to the underlying concentration of AgNPs in the solution. Typically, single-impact recordings are carried out in experimentally controlled media.<sup>[37,38]</sup> Yet, recent work demonstrated that it is also possible to measure in sea, bottled or tap water.<sup>[39–41]</sup> Moreover, impact electrochemistry is able to quantify samples containing unknown concentrations of (differently-sized) AgNPs.<sup>[42,43]</sup> Such measurements are typically performed in a standard three-electrode setup.<sup>[33]</sup> Due to the small currents at play during individual impacts, however, this can be further simplified to a two-electrode setup.<sup>[44,45]</sup> Moreover, with the possibility of designing small and simple potentiostats,<sup>[46–51]</sup> developed using sensitive integrated-chips, nano-impact electrochemistry could become a promising technique for on-site quantification.

Traditionally, a single glassy carbon electrode is used for detection.<sup>[38]</sup> However, in order to improve statistical validity, parallel recordings from microelectrode arrays (MEAs) can be implemented.<sup>[37,44,45,52]</sup> MEAs are typically fabricated using classical clean-room lithography methods. This established technique allows well-defined electrode openings (e.g. in the low micrometer range) with inert metals such as platinum.<sup>[53]</sup> However, for environmental monitoring, cost-effective sensors are preferred mainly due to the volume of tests that need to be conducted. In addition, disposable or single-use sensors are desired for their easy-to-use, reliable, and fast response times.<sup>[54]</sup> To this end, screen-printing is a promising additive manufacturing process capable to go roll-to-roll whilst limiting the amount of wasted material.<sup>[55,56]</sup> For example, heavy metal ions such as arsenic, cadmium, lead, and mercury have been detected via screen-printed electrodes (SPEs) for environmental monitoring.<sup>[22–26]</sup> Generally, SPEs tend to be quite large, ranging from a few mm to as low as 100  $\mu\text{m}$  in diameter.<sup>[57–60]</sup> Due to their large size and porosity (i.e. carbon, Pt, or Au), SPEs have quite low impedances in electrolyte media. For amperometric measurements this increases the current noise and ultimately obscures single nanoparticle impacts. This issue can be circumvented by limiting the electrode-electrolyte area by only pipetting a microliter sample onto the SPEs.<sup>[61]</sup> However, this is impractical for the end user and a more favorable approach would be to fabricate electrodes of smaller size via laser ablation.<sup>[62–65]</sup>

In this work, we investigate the use of screen-printed, laser-patterned microelectrode arrays (SPMEAs) for the electrochemical detection of AgNPs. In addition, we demonstrate the applicability of these sensors using an in-house built, portable nanoparticle detection (POND) device for detecting AgNPs contaminated with urea. Our method presents itself as a cost-effective platform for on-site monitoring of AgNPs via direct nano-impact electrochemistry.

## 2. Screen-Printed MEAs

In order to detect nanoparticles for future on-site applications, screen-printed microelectrode arrays (SPMEAs) were

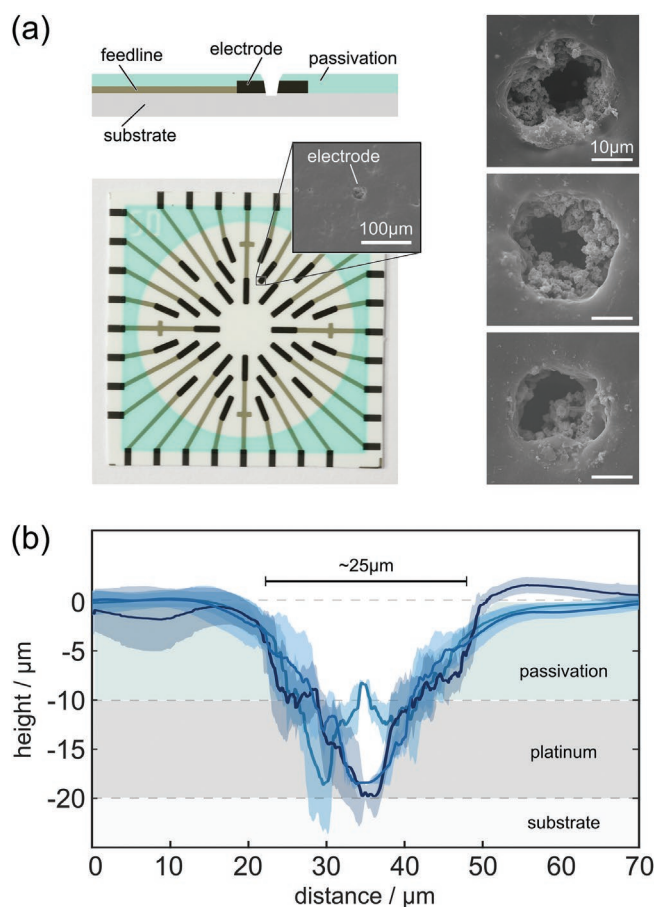


**Figure 1.** SPMEA for nano-impact electrochemistry. a) Schematic, optical, and SEM images of a laser-patterned screen-printed MEA (size  $24.15 \times 24.15$  mm). b) Average cross-sectional profiles of the three electrodes displayed in (a). The mean and standard deviation were calculated using six cross-sectional profiles  $30^\circ$  apart from each other.

fabricated via screen-printing and subsequent laser patterning, see **Figure 1**. In principle, three different electrode geometries – a disk electrode,<sup>[64]</sup> a recessed electrode,<sup>[65]</sup> and a ring electrode<sup>[62,63]</sup> – are possible with the laser ablation technique. The electrode radius  $r$  and the depth of ablation is primarily determined by the laser's pulse energy, pulse width, wavelength, focal area, and the number of pulses. In addition, the passivation's absorption characteristics and layer height will also influence the electrodes' final geometry. Therefore, to yield electrode geometries with only little dependence on the laser process, we tuned the parameter toward full penetration of the Pt layer. We obtained SPMEAs with 32 individually addressable electrodes which are hollow and  $\approx 12.5$   $\mu\text{m}$  in radius (view **Figure 1a,b**). In this case, the electrode size is mainly governed by the screen-printed layer height and electrode impedances suitable for single-impact electrochemical experiments can be achieved.

Nevertheless, after the laser patterning, it is important to clean the SPMEAs of process residues in order to expose active electrode sites.<sup>[66,67]</sup> These residues could be for example left-over binder components or potential oxide layers that arose due to laser ablation. Platinum oxide layers can be electrochemically reduced by using strong alkaline solutions such as KOH.<sup>[68]</sup>

However, in the case of screen-printed microelectrodes, we observed larger capacitive currents once they were activated in 100 mM KOH (see Supporting Information), most likely due to over etching and critical removal of the passivation layer.<sup>[69]</sup> This ultimately leads to a large electrode-electrolyte interface and consequent masking of the individual single nanoparticle impacts by the increased noise. In contrast, we observed a gradual but continuous activation for cyclic voltammetry cleaning in 0.2 M sulfuric acid (see **Figure 2a**). After 100 cycles, it was possible to see the characteristic oxidation and reduction of Pt in sulfuric acid as shown similarly in the literature.<sup>[70,71]</sup>

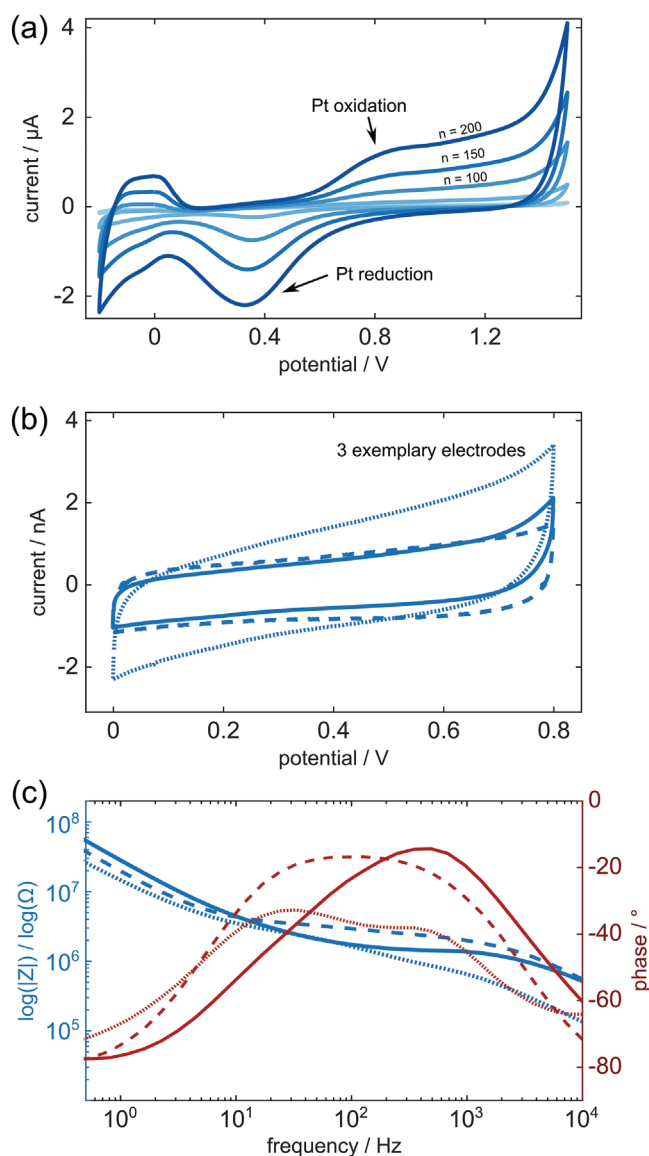


**Figure 2.** Electrochemical Characterization. a) Activation in 200 mM H<sub>2</sub>SO<sub>4</sub> solution. All electrodes were short-circuited during the activation (potential range  $-0.2$  to  $1.5$  V,  $500$  mV s<sup>-1</sup> scan rate, 200 cycles). The graph shows every 50th cycle. b) Cyclic voltammetry (0 to 800 mV,  $100$  mV s<sup>-1</sup> scan rate, 2nd cycle) of individual electrodes (solid, dashed, and dotted) and c) impedance spectroscopy (at  $0.18 \pm 0.01$  V) in PBS solution containing  $1$  mM ferri/ferrocyanide.

Once the SPMEA was activated, we rinsed the chips with deionized water and individually characterized representative electrodes with a redox-active tracer ( $1$  mM ferri/ferrocyanide in phosphate-buffered saline). Exemplary cyclic voltammograms are shown in **Figure 2b**, displaying a clear capacitive nature. We associate this capacitive behavior primarily to the electrodes' porous composite material which is known to form distributed contact impedances.<sup>[72]</sup> This is also confirmed by the impedance spectroscopy data shown in **Figure 2c** which displays a combination of RC elements (view plateau visible at  $\approx 100$  Hz). Inter-electrode variations are most likely explained by slight variations in the manufacturing process.

### 3. Nano-Impact Electrochemistry

After activation of the SPMEAs, we performed nano-impact experiments using  $20$  nm-sized citrate-capped AgNPs. Exemplary raw current traces are shown in **Figure 3** for  $200$  pM AgNPs in  $25$  mM KCl solution. The electrodes were biased to  $800$  mV vs. Ag/AgCl to ensure a maximum yield and the particles were inserted at  $\approx 45$  s. The data shows a clear difference between a solution containing pure electrolyte ( $t < 45$  s) and the AgNP-spiked solution ( $t > 50$  s). In fact, the current peaks associated with collision events exceed the RMS noise floor of  $77 \pm 2.3$  pA noticeably. We further applied a channel-specific threshold to extract the AgNP impacts that are considered in the subsequent analysis (visualized as blue dots) and measured an impact rate of  $4 \pm 1$  Hz ( $200$  pM AgNPs in  $25$  mM KCl). This value is in the same range as values reported for clean-room fabricated MEAs.<sup>[45,52]</sup> Hence, we conclude that the oxide layer at the electrode was successfully removed during the activation step. Thus, we expect SPMEAs to be suitable for quantitative AgNP detection.

To test this, we conducted nano-impact experiments with various particle concentrations in the pM-range and obtained an approximately linear relationship of  $22$  mHz pM<sup>-1</sup> between the impact rate and the underlying concentration, see **Figure 4**. Moreover, we were able to detect AgNP impacts at low concentrations of  $1$  pM.

#### 3.1. Towards On-Site Nanoparticle-Detection Using A Portable Device

We believe that nano-impact electrochemistry is a promising candidate to bridge the gap from the laboratory towards a highly sensitive yet cost-effective sensing technique for on-site applications.<sup>[73–75]</sup> To date, there are no commercially available portable multichannel amperometric systems dedicated for detecting AgNPs via impact electrochemistry. Therefore, we developed a portable nanoparticle detection (POND) device (see **Figure 5a**) that can be used for contamination sensing in-field. Our prototype can be connected to a notebook and directly used for pA-measurements. It supports parallel recordings from  $8$  channels, each at  $20$  kHz sampling rate (additional information can be found in the supplementary), and shielded from unwanted noise.

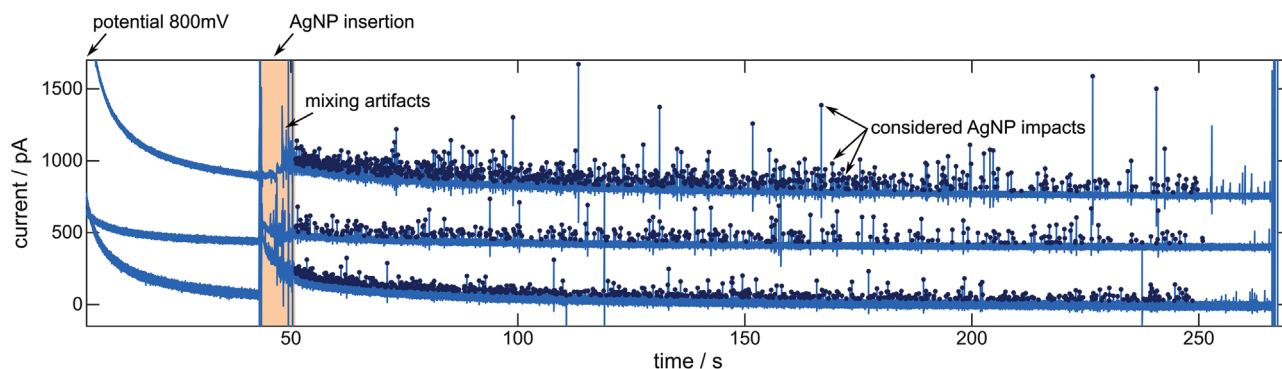


**Figure 3.** Single-impact experiment using 30 mM KCl solution containing 200 pM AgNP with 20 nm diameter. Current traces of three electrodes biased to 800 mV vs Ag/AgCl throughout the experiment. The particles were added and mixed (orange shading). Blue dots mark current peaks that are considered as AgNP impacts. Traces are shifted by 500 pA relative to one another for visual clarity.

To test the POND device in a simulated on-site environment, preliminary experiments were done in controlled media as similarly described (data not shown). Thereafter, we performed an initial proof-of-concept and detected AgNP in urea-spiked electrolyte solution using the 8-channel POND system. Since urea is typically present in natural (waste) water, we were interested in investigating their effect on our detection method. This study is to the best of our knowledge, the first attempt where a portable device was used to record nano-impacts on a low-cost MEA chip on-site. An exemplary current trace of a single electrode is provided in Figure 5b. The background noise in Figure 5b ( $\approx 13$  pA) can be attributed to weakly-shielded electronic circuits, as the cover of the device was left open during the measurement (to be able to insert the urea). Nevertheless, the current peaks upon collisions are clearly distinguishable from background noise – even after polluting the solution with urea.

Even in this non-ideal situation, we were generally able to differentiate particle impacts from noise by simple thresholding and obtained estimated particles sizes ( $19.0 \pm 2.4$  nm and  $19.3 \pm 2.9$  nm with and without urea pollution) that are similar to the expected value of 20 nm.

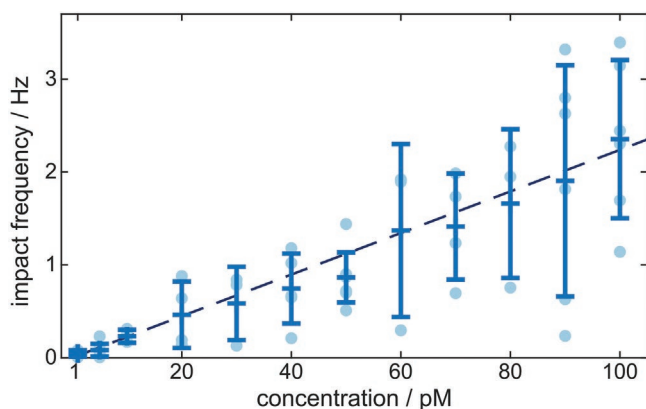


**Figure 4.** Impact frequency as a function of AgNP concentration. All experiments used an oxidation potential of 800 mV vs Ag/AgCl and were taken in 30 mM KCl solution. The data is based on the first 200 s after mixing. The dashed linear fit has a value of  $22 \text{ mHz pM}^{-1}$ . The impact frequencies of individual electrode channels are represented as circular dots. The error bars indicate standard deviation.

The data in Figure 5b also indicates that moderate amounts of urea do not critically interfere with the detection, since the number of current spikes is not drastically reduced after pollution. In fact, we observed a minor change from 1.0 Hz before pollution to 0.86 Hz afterward for the data in Figure 5. Moreover, the difference in impact rate might be also explained by dilution effects as well as differences in the diffusive mass transport, as there is typically a strong initial decrease after the potential application.

#### 4. Conclusion

We demonstrated the use of screen-printed, laser-patterned microelectrode arrays (SPMEAs) for detecting 20 nm diameter silver nanoparticles (AgNPs) via nano-impact electrochemistry. By simple laser ablation through the electrode material, electrodes were formed allowing pA current transients to be measured after cleaning. With our 64-channel lab-based amplifier system, we were able to obtain a linear relationship between the impact frequency and the AgNP concentration ( $22 \text{ mHz pM}^{-1}$ ,  $R^2 = 97.6\%$ ). This allows future unknown concentrations of AgNPs to be identified using our SPMEAs. In order to go towards more real-world measurements, an on-site portable nanoparticle detection (POND) device was built. Its capability under on-site constraints was exemplarily demonstrated during a pollution-experiment, where we recorded impacts with our low-cost platform. Faradaic nano-impacts were detected, before and after the addition of urea, with marginal changes to their measured size. We also believe a similar setup could be of use in directly detecting other metals such as Ni or Cu nanoparticles.<sup>[42,76,77]</sup> However, careful consideration to the electrode's material, electrolyte composition, and applied potential is required. In summary, we believe this simple and cost-effective SPMEA coupled with a POND-like device would allow more rapid on-site monitoring of potentially contaminated AgNP environments.

#### 5. Experimental Section

**Chemicals:** Silver nanoparticles (mean size 20 nm,  $0.02 \text{ mg mL}^{-1}$  in aqueous solution), sulfuric acid ( $\text{H}_2\text{SO}_4$ , 95%–98%), urea, potassium chloride (KCl), potassium ferricyanide, potassium ferrocyanide, and

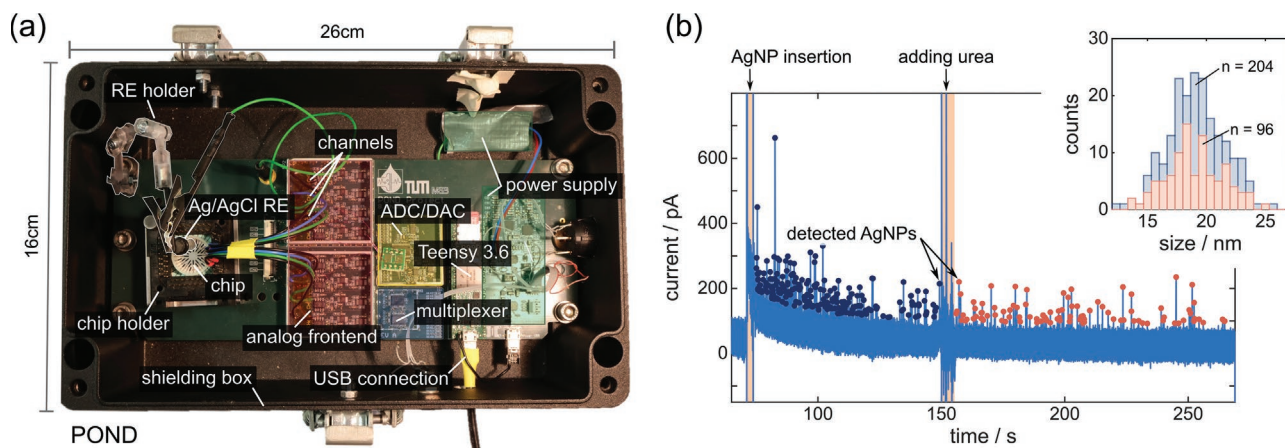


**Figure 5.** On-site AgNP detection using the in-house built portable nanoparticle detection (POND) device for a waste-water mimicking experiment. a) Schematic of the POND device that is able to record simultaneously from 8 channels at a sampling rate 20 kHz. b) Raw data of a single electrode for 223 pM AgNP in 30 mM KCl. After 150 s, the solution was polluted with 10  $\mu$ M urea simulating a typical contaminant in waste water.

modified phosphate-buffered saline (PBS) solution were purchased from Merck, Germany. All dilutions were prepared using deionized water from a BerryPURE purification system (Berrytec GmbH, Germany).

**Screen-Printed Microelectrode Arrays:** The screen-printed microelectrode arrays (SPMEAs) were fabricated on commercial polyester substrates (Melinex 339, Dupont Teijin Films, Wilton, UK) using a semi-automatic screen-printer (EKRA X5, Scanditron, Spånga, Sweden). The screen characteristics regarding mesh count and emulsion thickness were selected in accordance with the specifications of the ink manufacturers.

The fabrication of the SPMEAs consists of six individual layers printed subsequently with a drying step after each print. The feedlines were printed using a silver-based ink (Smart Screen F (S-CS21303), GenesInk, Rousset, France) and covered with carbon ink (Loctite EDAG 423 SS, Henkel, California, USA) at the contact areas. Platinum ink (BQ-321, DuPont, Bristol, UK) was used at the electrode site. In order to cover the printed features, a transparent dielectric ink (Luxprint 7165, DuPont, Bristol, UK) was printed twice to minimize the risk of pinholes. Finally, an encapsulation ink (Loctite EDAG 452SS Henkel, California, USA) was printed as an additional flow stop boundary. Solvent-based inks were dried using a conveyor belt oven set to 120  $^{\circ}$ C with a speed of 4 m  $\text{min}^{-1}$ . The overall heat-treatment procedure lasts for about 2 min. The UV-ink was cured with a dose of  $\approx 0.7$  J  $\text{cm}^{-2}$ .

A three-axis UV laser marker (MD-U1000C, Keyence, Osaka, Japan) was used to cut a 20  $\mu$ m hole through the passivation layer, exposing the conductive Pt layer. A two-step laser procedure was used. For the first laser step, the system was set to 10 kW, with a filling interval of 4  $\mu$ m, and only repeated once. The second laser setting was repeated 100 times as a polishing step, with the laser set to 0.2 kW and a filling interval of 2  $\mu$ m. Both used a shutter frequency of 400 kHz, writing at a speed of 1 m  $\text{s}^{-1}$ .

Glass rings were glued onto the SPMEAs and served as fluid reservoirs. They had a height and inner diameter of 10 mm and 17 mm, respectively.

**Electrochemical Experiments:** The electrochemical activation and the electrode characterization were performed with a VSP-300 potentiostat (Bio-Logic Science Instruments, Seyssinet-Pariset, France) in a three-electrode configuration with a flexible Ag/AgCl reference (Dri-Ref, Flexref from World Precision Instruments, Sarasota, USA) and a coiled platinum wire counter electrode. To initially clean and activate the electrode surface, a cyclic voltammetry (CV) step from  $-0.2$  to 1.5 V with a scan rate of 500 mV  $\text{s}^{-1}$  and 200 cycles was performed in 200 mM  $\text{H}_2\text{SO}_4$ . Prior to the detection experiments, the chips were additionally cleaned by thoroughly rinsing with deionized water and applying another short electrochemical activation: CV in  $\text{H}_2\text{SO}_4$  with 20 cycles.

The characterization of the individual electrodes was performed in modified PBS solution that contained 1 mM ferricyanide and 1 mM ferrocyanide as redox couple. Here, a CV (potential range from 0 to 0.8 V, 50 mV  $\text{s}^{-1}$  scan rate, 2nd cycle evaluated) and a subsequent impedance spectroscopy (PEIS, frequency range 0.5 Hz to 10 kHz, applied potential  $0.18 \pm 0.01$  V) was carried out for each electrode. In total, 20 electrodes from 2 chips were analyzed.

The silver nanoparticle calibration measurements were performed in a shielded and vibration-dampened environment, using a two-electrode setup. An inhouse-built transimpedance amplifier system that is able to record 64 channels in parallel at 10 kHz was used (3.4 kHz bandwidth) to obtain the calibration curve.<sup>[44,45,78]</sup> In these experiments a Ag/AgCl from BaSi (RE-4, 3 M NaCl gel electrode) served as reference. All measurements used 30 mM of KCl solution with a total volume of 700  $\mu$ L. The AgNPs were directly added from stock solution after biasing the electrodes to the oxidation potential of 800 mV vs Ag/AgCl. Then, the solution was mixed by pipetting 500  $\mu$ L volume in and out three times (within  $\approx 5$  to 10 s) and AgNP impacts were recorded. The total analysis time was 200 s.

The contamination experiment was carried out in an in-house built portable nanoparticle detection (POND) device that features 8 channels in a two-electrode configuration (further information see Supporting Information). In this experiment, Faradaic nano-impacts from 200 pM AgNP in 30 mM KCl were recorded after direct pipetting and mixing. After an initial recording phase, the solution was contaminated by adding 100  $\mu$ L of 1 mM urea while the potential was kept at 800 mV vs Ag/AgCl.

**Scanning Electron Microscopy:** The screen-printed microelectrode array (SPMEA) was sputtered with  $\approx 10$  nm of Au (5 Pa, 40 s, 40 mA) using a high-vacuum coating system (BAL-TEC Med 020, LabMakelaar Benelux BV, The Netherlands). Copper tape and conductive double sided carbon-tab was used to fix the SPMEA to the holder to prevent charge accumulation. All scanning electron images were taken using a scanning electron microscope (JSM-6060LV, JEOL, Tokyo, Japan) at an acceleration voltage of 15 kV, a magnification of 100 $\times$  or 2500 $\times$ , and a substrate tilt of 0 $^{\circ}$ .

**Optical Profilometry:** Already sputtered screen-printed microelectrodes were measured using a 3D laser scanning confocal microscope (VK-X250, Keyence, Osaka, Japan) in combination with a 150 $\times$  objective (150 $\times$ /0.95 CF Plan Apo OFN25, Nikon, Japan). A high and low laser intensity (double-scan feature) was used on each individual microelectrode in order to evaluate its morphology. The neutral density filter of the microscope was automatically calibrated (auto gain function) after setting the lower and upper limits of the scan. A z-pitch of 80 nm was used for each measurement, that was carried out

on a vibration-dampened table (Vision IsoStation, Newport Corporation, California, USA) to reduce external interferences.

**Data Processing:** The data was processed via a custom algorithm in Matlab, similar to previous work.<sup>[52]</sup> First, channels that show noisy as well as unresponsive electrodes were excluded. Then all raw traces were de-trended to account for low-frequency relaxation of the background current. The AgNP impacts were identified via current thresholding. Here, a channel-specific threshold was set ( $0.5 i_{pk2pk} + 5$  pA) by considering the individual peak-to-peak background noise ( $i_{pk2pk}$ ). Depending on the capacitive load of each electrode, amplifier related ringing-artifacts can be observed after the initial charge injection caused by an impacting AgNP. These artifacts were excluded by setting a minimum inter-peak distance of 10 ms. The results shown above are based on recordings from  $n \geq 6$  electrodes per concentration, acquired from two different chips.

Profilometric data was evaluated using MultiFileAnalyzer software (Keyence, Osaka, Japan). Background subtraction was manually set around the electrode opening using a 2D polynomial of order one in  $x$  and  $y$ . Within the software, six individual profiles were taken at  $30^\circ$  intervals (see Supporting Information). These profiles were later averaged in Matlab displaying the mean and standard deviation.

## Supporting Information

Supporting Information is available from the Wiley Online Library or from the author.

## Acknowledgements

L.Grob and L.J.K.Weiß contributed equally to this work. We greatly appreciate Dr.-Ing. Bernhard Gleich for his advice during the development of the portable nanoparticle detection (POND) device. In addition, we wish to thank Jonathan Rapp, Handenur Çalıřkan, Firas Labidi, and Oscar Soto Rivera for their aid in developing the different modules used in the final device. L. Grob and I. Schwertfeger acknowledged the financial aid received from the German Federal Ministry for Economic Affairs and Climate Action via a ZIM-cooperation-project (ZF4730901SA9). L. J. K. Weiß and E. Music greatly appreciated funding from the German Research Foundation (DFG, grant number 446370753), G. Al Boustani and M. Nikić acknowledge funding from the Dobeneck-Technologie-Stiftung and the IGSTC/BMBF (grant number 01DQ21003B), respectively.

Open access funding enabled and organized by Projekt DEAL.

## Conflict of Interest

The authors declare no conflict of interest.

## Data Availability Statement

The data that support the findings of this study are available from the corresponding author upon reasonable request.

## Keywords

impact electrochemistry, screen-printed microelectrodes, silver nanoparticles, laser ablation, point-of-use

Received: November 5, 2022

Revised: January 18, 2023

Published online: February 5, 2023

- [1] K. Schmid, M. Riediker, *Environ. Sci. Technol.* **2008**, *42*, 2253.
- [2] R. Kessler, *Environ. Health Perspect.* **2011**, *119*, A120.
- [3] M. E. Vance, T. Kuiken, E. P. Vejerano, S. P. McGinnis, M. F. Hochella, D. Rejeski, M. S. Hull, *Beilstein J. Nanotechnol.* **2015**, *6*, 1769.
- [4] S. F. Hansen, L. R. Heggelund, P. R. Besora, A. Mackevica, A. Boldrin, A. Baun, *Environ Sci: Nano* **2016**, *3*, 169.
- [5] N. Savage, M. S. Diallo, *J Nanopart Res* **2005**, *7*, 331.
- [6] B. C. Englert, *J Environ Monit* **2007**, *9*, 1154.
- [7] E. McGillicuddy, I. Murray, S. Kavanagh, L. Morrison, A. Fogarty, M. Cormican, P. Dockery, M. Prendergast, N. Rowan, D. Morris, *Sci. Total Environ.* **2017**, *575*, 231.
- [8] M. Rai, A. Yadav, A. Gade, *Biotechnol. Adv.* **2009**, *27*, 76.
- [9] B. Nowack, H. F. Krug, M. Height, *Environ. Sci. Technol.* **2011**, *45*, 1177.
- [10] C. A. Dos Santos, M. M. Seckler, A. P. Ingle, I. Gupta, S. Galdiero, M. Galdiero, A. Gade, M. Rai, *J. Pharm. Sci.* **2014**, *103*, 1931.
- [11] V. De Matteis, M. A. Malvindi, A. Galeone, V. Brunetti, E. De Luca, S. Kote, P. Kshirsagar, S. Sabella, G. Bardi, P. P. Pompa, *Nanomedicine* **2015**, *11*, 731.
- [12] R. de Lima, A. B. Seabra, N. Durán, *J. Appl. Toxicol.* **2012**, *32*, 867.
- [13] P. V. AshaRani, G. Low Kah Mun, M. P. Hande, S. Valiyaveetil, *ACS Nano* **2009**, *3*, 279.
- [14] T.-H. Kim, M. Kim, H.-S. Park, U. S. Shin, M.-S. Gong, H.-W. Kim, *J. Biomed. Mater. Res.* **2012**, *100A*, 1033.
- [15] A. R. Gliga, S. Skoglund, I. Odnevall Wallinder, B. Fadeel, H. L. Karlsson, *Part. Fibre Toxicol.* **2014**, *11*, 11.
- [16] L. R. R. Souza, V. S. da Silva, L. P. Franchi, T. A. J. de Souza, in *Cellular and Molecular Toxicology of Nanoparticles* (Eds: Q. Saquib, M. Faisal, A. A. Al-Khedhairi, A. A. Alatar), Springer International Publishing, Cham **2018**, pp. 251–262.
- [17] L. Degenkolb, F. Leuther, S. Lüderwald, A. Philippe, G. Metreveli, S. Amininejad, H.-J. Vogel, M. Kaupenjohann, S. Klitzke, *Sci. Total Environ.* **2020**, *699*, 134387.
- [18] J.-L. Wang, E. Alasonati, M. Tharaud, A. Gelabert, P. Fiscaro, M. F. Benedetti, *Water Res.* **2020**, *176*, 115722.
- [19] J. Fabrega, S. N. Luoma, C. R. Tyler, T. S. Galloway, J. R. Lead, *Environ Int* **2011**, *37*, 517.
- [20] E. M. Heithmar, *Screening Methods for Metal-Containing Nanoparticles in Water*, U.S. Environmental Protection Agency, Washington, DC **2011**.
- [21] J. Liu, S. Yu, Y. Yin, J. Chao, *Trends Analyt Chem* **2012**, *33*, 95.
- [22] G. Hanrahan, D. G. Patil, J. Wang, *J Environ Monit* **2004**, *6*, 657.
- [23] M. Li, Y.-T. Li, D.-W. Li, Y.-T. Long, *Anal. Chim. Acta* **2012**, *734*, 31.
- [24] A. Hayat, J. L. Marty, *Sensors* **2014**, *14*, 10432.
- [25] J. Barton, M. B. G. Garcia, D. H. Santos, P. Fanjul-Bolado, A. Ribotti, M. McCaul, D. Diamond, P. Magni, *Microchim. Acta* **2016**, *183*, 503.
- [26] M. Li, D.-W. Li, G. Xiu, Y.-T. Long, *Curr. Opin. Electrochem.* **2017**, *3*, 137.
- [27] E. Bernalte, S. Arévalo, J. Pérez-Taborda, J. Wenk, P. Estrela, A. Avila, M. Di Lorenzo, *Sens. Actuators, B* **2020**, *307*, 127620.
- [28] M. C. Stensberg, Q. Wei, E. S. McLamore, D. M. Porterfield, A. Wei, M. S. Sepúlveda, *Nanomedicine* **2011**, *6*, 879.
- [29] Z. Ferdous, A. Nemmar, *Int. J. Mol. Sci.* **2020**, *21*, 2375.
- [30] S. Garcia-Segura, X. Qu, P. J. J. Alvarez, B. P. Chaplin, W. Chen, J. C. Crittenden, Y. Feng, G. Gao, Z. He, C.-H. Hou, X. Hu, G. Jiang, J.-H. Kim, J. Li, Q. Li, J. Ma, J. Ma, A. B. Nienhauser, J. Niu, B. Pan, X. Quan, F. Ronzani, D. Villagran, T. D. Waite, W. S. Walker, C. Wang, M. S. Wong, P. Westerhoff, *Environ. Sci.: Nano* **2020**, *7*, 2178.
- [31] A. Sekretareva, *Sens Actuators Rep* **2021**, *3*, 100037.
- [32] K. E. Fink, B. J. Polzin, J. T. Vaughey, J. J. Major, A. R. Dunlop, S. E. Trask, G. T. Jeka, J. S. Spangenberg, M. A. Keyser, *J. Power Sources* **2022**, *518*, 230760.

- [33] S. V. Sokolov, S. Eloul, E. Kätelhön, C. Batchelor-McAuley, R. G. Compton, *Phys. Chem. Chem. Phys.* **2017**, *19*, 28.
- [34] Y.-Y. Peng, R.-C. Qian, M. E. Hafez, Y.-T. Long, *ChemElectroChem* **2017**, *4*, 977.
- [35] F. T. Patrice, K. Qiu, Y.-L. Ying, Y.-T. Long, *Annu. Rev. Anal. Chem.* **2019**, *12*, 347.
- [36] P. A. Defnet, T. J. Anderson, B. Zhang, *Curr. Opin. Electrochem.* **2020**, *22*, 129.
- [37] K. J. Krause, F. Brings, J. Schnitker, E. Kätelhön, P. Rinklin, D. Mayer, R. G. Compton, S. G. Lemay, A. Offenhäusser, B. Wolftrum, *Chemistry* **2017**, *23*, 4638.
- [38] Y.-G. Zhou, N. V. Rees, R. G. Compton, *Angew. Chem., Int. Ed.* **2011**, *50*, 4219.
- [39] E. J. E. Stuart, N. V. Rees, J. T. Cullen, R. G. Compton, *Nanoscale* **2013**, *5*, 174.
- [40] E. J. E. Stuart, K. Tschulik, D. Omanović, J. T. Cullen, K. Jurkschat, A. Crossley, R. G. Compton, *Nanotechnology* **2013**, *24*, 444002.
- [41] X. Li, C. Batchelor-McAuley, R. G. Compton, *ACS Sens.* **2019**, *4*, 464.
- [42] E. J. E. Stuart, Y.-G. Zhou, N. V. Rees, R. G. Compton, *RSC Adv.* **2012**, *2*, 6879.
- [43] P. Béltéky, A. Rónavári, N. Igaz, B. Szerencsés, I. Y. Tóth, I. Pfeiffer, M. Kiricsi, Z. Kónya, *Int J Nanomedicine* **2019**, *14*, 667.
- [44] K. J. Krause, A. Yakushenko, B. Wolftrum, *Anal. Chem.* **2015**, *87*, 7321.
- [45] P. G. Figueiredo, L. Grob, P. Rinklin, K. J. Krause, B. Wolftrum, *ACS Sens.* **2018**, *3*, 93.
- [46] J. L. Delaney, E. H. Doeven, A. J. Harsant, C. F. Hogan, *Anal. Chim. Acta* **2013**, *790*, 56.
- [47] M. D. Steinberg, P. Kassal, I. Kereković, I. M. Steinberg, *Talanta* **2015**, *143*, 178.
- [48] E. H. Doeven, G. J. Barbante, A. J. Harsant, P. S. Donnelly, T. U. Connell, C. F. Hogan, P. S. Francis, *Sens. Actuators, B* **2015**, *216*, 608.
- [49] A. Ainla, M. P. S. Mousavi, M.-N. Tsaloglou, J. Redston, J. G. Bell, M. T. Fernández-Abedul, G. M. Whitesides, *Anal. Chem.* **2018**, *90*, 6240.
- [50] A. W. Colburn, K. J. Levey, D. O'Hare, J. V. Macpherson, *Phys. Chem. Chem. Phys.* **2021**, *23*, 8100.
- [51] R. B. Clark, M. W. Glasscott, M. D. Verber, J. C. DeMartino, A. Netchaev, J. D. Ray, E. W. Brown, E. Alberts, P. U. A. I. Fernando, L. C. Moores, J. E. Dick, *Anal. Chem.* **2021**, *93*, 7381.
- [52] L. J. K. Weiß, E. Music, P. Rinklin, L. Straumann, L. Grob, D. Mayer, B. Wolftrum, *ACS Appl. Nano Mater.* **2021**, *4*, 8314.
- [53] L. R. Grob, *Printed 3D Electrodes for Sensing and Bioelectronics*, Technische Universität, München **2021**.
- [54] C. Dincer, R. Bruch, E. Costa-Rama, M. T. Fernández-Abedul, A. Merkoçi, A. Manz, G. A. Urban, F. Güder, *Adv. Mater.* **2019**, *31*, 1806739.
- [55] R. Søndergaard, M. Hösel, D. Angmo, T. T. Larsen-Olsen, F. C. Krebs, *Mater. Today* **2012**, *15*, 36.
- [56] L. Hakola, E. Jansson, R. Futsch, T. Happonen, V. Thenot, G. Depres, A. Rougier, M. Smolander, *Int J Adv Manuf Technol* **2021**, *117*, 2921.
- [57] S. Laschi, I. Palchetti, G. Marrazza, M. Mascini, *J. Electroanal. Chem.* **2006**, *593*, 211.
- [58] R. O. Kadara, N. Jenkinson, C. E. Banks, *Electrochem. Commun.* **2009**, *11*, 1377.
- [59] R. O. Kadara, N. Jenkinson, C. E. Banks, *Sens. Actuators, B* **2009**, *142*, 342.
- [60] F. Tan, J. P. Metters, C. E. Banks, *Sens. Actuators, B* **2013**, *181*, 454.
- [61] M. Z. M. Nasir, M. Pumera, *Phys. Chem. Chem. Phys.* **2016**, *18*, 28183.
- [62] J. C. Ball, J. K. Lumpp, S. Daunert, L. G. Bachas, *Electroanalysis* **2000**, *12*, 685.
- [63] J. C. Ball, D. L. Scott, J. K. Lumpp, S. Daunert, J. Wang, L. G. Bachas, *Anal. Chem.* **2000**, *72*, 497.
- [64] C. Cugnet, O. Zaouak, A. René, C. Pécheyran, M. Potin-Gautier, L. Authier, *Sens. Actuators, B* **2009**, *143*, 158.
- [65] S. Liébana, L. J. Jones, G. A. Drago, R. W. Pittson, D. Liu, W. Perrie, J. P. Hart, *Sens. Actuators, B* **2016**, *231*, 384.
- [66] J. P. Metters, R. O. Kadara, C. E. Banks, *Analyst* **2011**, *136*, 1067.
- [67] H. Wan, Q. Sun, H. Li, F. Sun, N. Hu, P. Wang, *Sens. Actuators, B* **2015**, *209*, 336.
- [68] S.-M. Park, S. Ho, S. Aruliah, M. F. Weber, C. A. Ward, R. D. Venter, S. Srinivasan, *J. Electrochem. Soc.* **1986**, *133*, 1641.
- [69] J. Lee, D. W. M. Arrigan, D. S. Silvester, *Sens. Biosensing Res* **2016**, *9*, 38.
- [70] Y. Sugawara, T. Okayasu, A. P. Yadav, A. Nishikata, T. Tsuru, *J. Electrochem. Soc.* **2012**, *159*, F779.
- [71] L. Jacobse, S. J. Raaijman, M. T. M. Koper, *Phys. Chem. Chem. Phys.* **2016**, *18*, 28451.
- [72] S. Zips, L. Grob, P. Rinklin, K. Terkan, N. Y. Adly, L. J. K. Weiß, D. Mayer, B. Wolftrum, *ACS Appl. Mater. Interfaces* **2019**, *11*, 32778.
- [73] L. M. Furtado, M. Bundschuh, C. D. Metcalfe, *Bull. Environ. Contam. Toxicol.* **2016**, *97*, 449.
- [74] A. Syafuddin, S. Salmiati, T. Hadibarata, A. B. H. Kueh, M. R. Salim, M. A. A. Zaini, *Sci. Rep.* **2018**, *8*, 986.
- [75] M. Millour, J.-P. Gagné, K. Doiron, I. Marcotte, A. A. Arnold, É. Pelletier, *Colloids Surf. A* **2021**, *623*, 126767.
- [76] Y.-G. Zhou, B. Haddou, N. V. Rees, R. G. Compton, *Phys. Chem. Chem. Phys.* **2012**, *14*, 14354.
- [77] B. Haddou, N. V. Rees, R. G. Compton, *Phys. Chem. Chem. Phys.* **2012**, *14*, 13612.
- [78] A. Yakushenko, E. Kätelhön, B. Wolftrum, *Anal. Chem.* **2013**, *85*, 5483.